National Conference with International Participation
ENGINEERING MECHANICS 2006
Svratka, Czech Republic, May 15 – 18, 2006
paper no. 325

MONOLENS SYSTEM FOR BUBBLE DIMENSION AND POSITION MEASUREMENT

J. Hošek*

Summary: *This paper presents a new optical system, which is able to determinate radius and position in 3D-observation space of a number of spherical bubbles with using the only one monolens camera system. The principle of the system is based on anamorphotic optical system and appropriate data processing algorithm. The precision and repeatability of the system were tested by measurement of a glass and steel sphere mounted on x, y, z movable support. The first measurement and data processing are demonstrated in multiphase bubble-liquid system. We expect the presented system will be able to be used for the determination of the objects velocity as well as dimension change in the case of application of time-resolved photography.*

1. Introduction

Determination of bubble objects in space is very important in many technical or production applications. Observation and determination of dimension and position of these objects can affect or be the bases for optimization of the technological processes like chemical reactors, where homogeneous distribution of bubbles is often demanded in multiphase reacting systems. On the other hand, there are technologies where the presence of multiphase system can indicate a technological problem, for example in hydrodynamic systems or in glass production industry. Bubble dimension and distribution measurement is important for the studies of environmental engineering too.

Different experimental systems, which allow determination of the position and radius of the bubbles, have been under development since the 1970s. There are many kinds of camera systems used for bubble properties measurement (Leifer *et al* 2003). A lot of experimental methods applied to bubble properties measurement is based on particle image velocimetry (PIV) systems (Hassan 1997), (Lindken, Merzkirch 2001) and others. It is necessary to use Stereo PIV based on two or more camera and laser systems for in 3D space measurement.

There are other more sophisticated systems still in development. The properties of bubbles can be measured with interference method application (Niwa *et al* 2000), laser light scattering method (Guerrero *et al* 2000) or holographic methods (Pu *et al* 2000), (Pan, Meng 2002). The main disadvantage of the referred methods is the necessity of using expensive devices like high speed or resolution cameras, laser systems or special experimental conditions. It decreases usage convenience of these methods for industrial and non scientific applications. Due to this fact new methods to determine bubble properties in 3D space measured with only one camera with simple illumination system were presented recently. These methods are based on numerical computation of position data from temporal (Szeliski, Kang 1993) or

* Ing. Jan Hošek, Ph.D. Department of Instrumentation and Control Engineering, Division of Precision Mechanics and Optics, Faculty of Mechanical Engineering, Czech Technical University in Prague, Technická 4, 166 07 Prague 6, Czech Republic, tel.: +420 224 352 552, e-mail: Jan.Hosek@fs.cvut.cz

optical information (Otero *et al* 2003) of the captured images. The most convenient method of bubble measurement for industrial and technical purposes seems to be the defocusing PIV method presented by (Willert, Gharib 1992) and developed to the digital method (DDPIV) applied to bubbly flows (Pereira *et al* 2000), (Jeon *et al* 2002). This method uses only one camera lens and mask with two or more apertures. The sensor is out of lens focusing plane, so that each light source gives the same number of spots on the sensor as the number of apertures used.

This paper presents a new optical system, which is able to determinate radius and position of a number of spherical bubbles in 3D-observation space using only one monolens camera system. The principle of the system is based on anamorphotic optical system and appropriate data processing algorithm.

2. Principle of the method

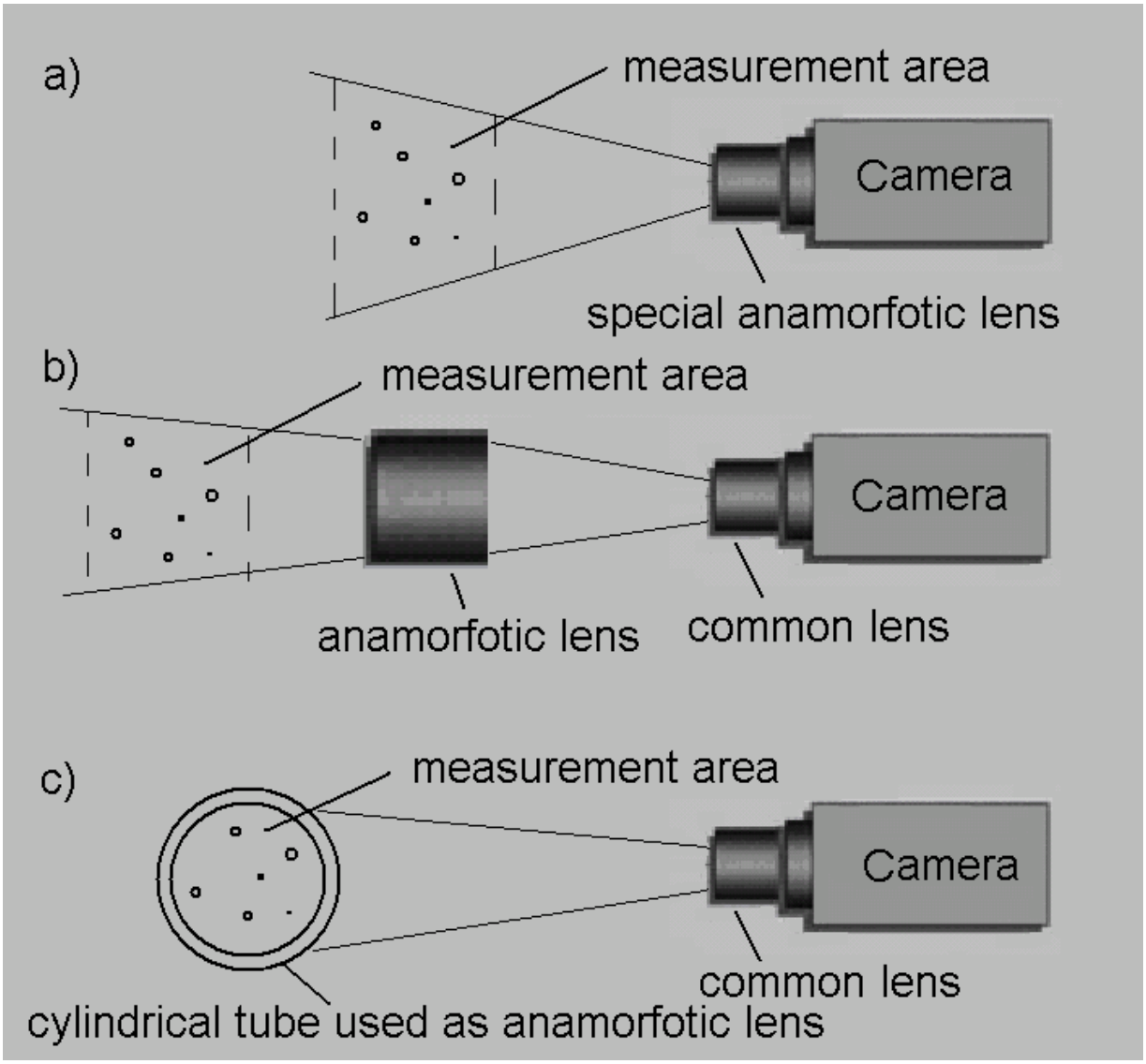

Figure 1 Three different instrument set-up of devised system.

Presented experimental method (Hošek 2006) is based on anamorphotic optical system and known shape of the measured object. Anamorphotic optical system is characterized with astigmatism - different magnification in different planes along the optical axis. The typical representative of the anamorphotic optical system is cylindrical lens. This system imagines the object with different magnification in different directions perpendicular to the optical axis. Due to the fact, that objects magnification is a function of the object distance it is possible to unambiguously determinate object distance from the ratio of magnifications different planes of anamorphotic system and direction to the object. For the image magnifications determination it is necessary to know the ratio of dimension of original object. This value is well known for the spherical objects, where the ratio of dimensions is equal to 1 in all directions.

This experimental method is able to be used for the measurement of all kinds of spherical objects. It can be bubbles in liquids, droplets in gases, droplets of different density in liquids or solid spheres in gases or liquids. Real measurement can be realized with three different kinds of experimental instruments. It can be used special anamorphotic lens instead of common camera lens. The second possibility is to use common camera lens and anamorphotic lens placed to the optical system. The third kind of set-up is to use the common camera lens and a cylindrical tube used as an anamorphotic lens. All three kinds of instrument set-up are shown in the figure 1.

This last mentioned set-up of the devised method seems to be the most profitable application in industry due to its easy installation, since the of majority of pipes in industry are of cylindrical tube shape and presented method employs this tube as a part of set-up. Optical scheme of this set-up is shown in the figure 2.

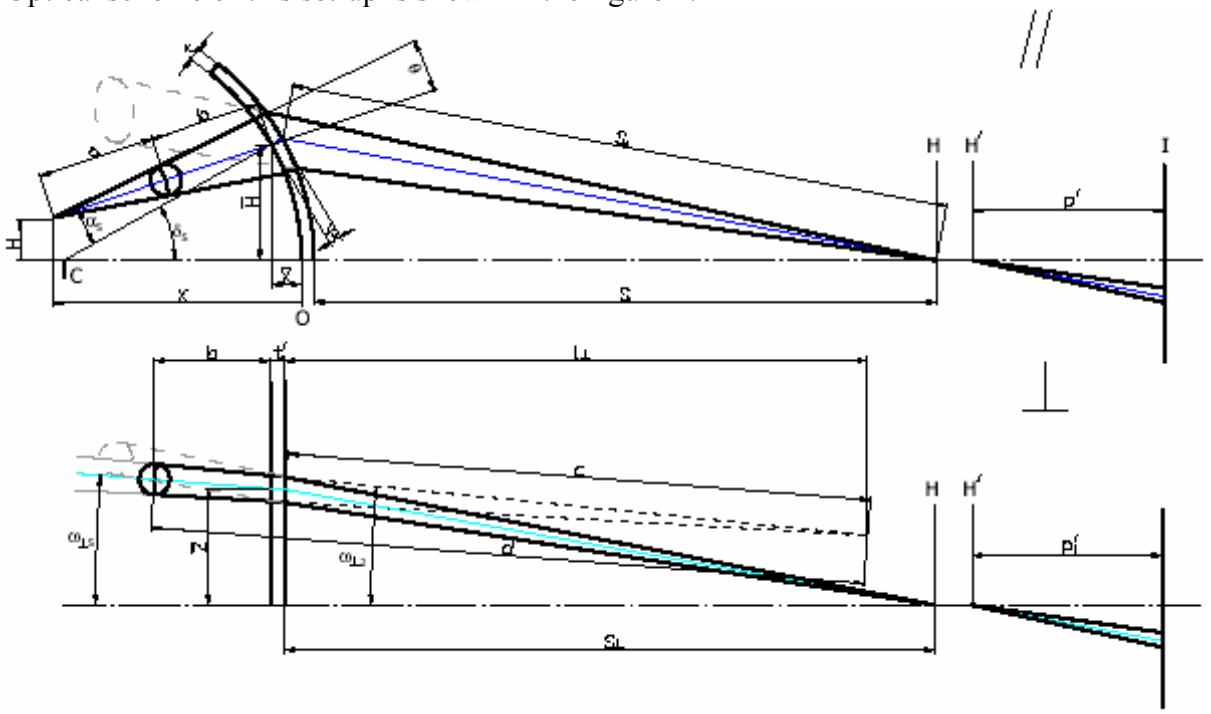

Figure 2 Optical scheme of the devised system with cylindrical tube set-up.

There are two views shown of the optical system. The upper one in the plain contains optical axis of the system, marked // and perpendicular to the cylindrical tube axis. There is shown the part of the tube on the left and camera system represented with main planes of the camera

lens H and H´ and image plane I on the right. The main rays corresponding to the bubble margin in this plane are depicted with black lines. The bottom part of the figure shows the main rays along the central – blue line in the plane perpendicular to the upper part plane, marked ⊥. The angles of the main rays are determined from the camera-captured image and position of each ray on the tube wall is computed with the basic geometrical optics. Angles marked ω are measured from optical axis, angles marked α are measured from normal and angles marked δ are measured around tube curvature centroid C. Distance of intersections of the main rays can be solved in both planes by equations:

$$a + b = \sqrt{\left(H - \overline{H}\right)^2 + \left(X - \overline{X}\right)^2} \tag{1}$$

$$d = \frac{b + l_{\perp}}{\cos \omega_{\perp S}} \tag{2}$$

It is easy to compute the radius of the sphere in both planes by:

$$R_{//} = a \sin \theta \tag{3}$$

$$R_{\perp} = d \sin(\omega_{\perp 2} - \omega_{\perp S}) \tag{4}$$

Spherical objects have constant radius in all directions, so that both radii have to be equal. Due to this condition the sphere radius and its position is computed by equations:

$$R = \frac{\sqrt{\left(H - \overline{H}\right)^2 + \left(X - \overline{X}\right)^2} + l_{\perp}}{\dfrac{1}{\sin \theta} + \dfrac{\cos \omega_{\perp S}}{\sin(\omega_{\perp 2} - \omega_{\perp S})}} . \tag{5}$$

$$X = \overline{X} + b \cos(\delta_S - \alpha_S) \tag{6}$$

$$Y = \overline{Y} + b \sin(\delta_S - \alpha_S) \tag{7}$$

$$Z = \overline{Z} + b \tan \omega_{\perp S} , \tag{8}$$

where

$$b = \frac{R \cos \omega_{\perp S}}{\sin(\omega_{\perp 2} - \omega_{\perp S})} - l_{\perp} . \tag{9}$$

Coordinate origin of determined sphere position lies in the intersection of the tube inner surface and system optical axis O.

The cylindrical tube serves like a magnifying glass in this set-up configuration due to the inner part of the tube lying in front of the rear focal plane of the tube. The tube imagines the bubble inside to the virtual magnified image and this image is observed with camera optics. Distance of the tube focal plane from the first tube wall can be determined with:

$$s_{F'} = \frac{n_3 n_2 r_1 r_2 - n_3 n_2 (n_2 - n_1) t}{n_2 r_2 (n_2 - n_1) + (n_3 - n_2)\left[n_2 r_1 - (n_2 - n_1) t\right]} , \tag{10}$$

where n_i are refractive indexes, r_i are curvature radii and t is tube wall thickness. This distance is always greater than tube diameter for glass tube of any diameter filled with water. This condition is fulfilled for the inert liquid refractive index up to 1,95 for 50 mm tube diameter. It means this method is suitable for any kind of liquid, high refractive indexes liquids or

melted glasses included. Cylindrical tube filled with a liquid of refractive index higher then air magnifies bubble image not only in one plane, but due to the refractive indexes difference in front of and behind the tube wall in both perpendicular planes. It contributes to better resolution of the measurement.

The main requirement to the camera detection system is the ability to establish bubble image margins. It means all bubble image has to be sharp enough for bubble margins determination. Every optical system is able to imagine sharply only objects lied in the limited distance called depth of field. Depth of field is given by:

$$\Delta = \frac{2Dgd_0}{D^2 - d_0^2} \ , \tag{11}$$

where D is entrance pupil diameter, d_0 is size of the accepted unsharpness in the object space and g is the object distance. It is necessary to set the object field of the optical system to contain virtual images of the bubble in both perpendicular planes.

3. Spherical bubbles

In general, bubbles are parts of different phases in liquids. They are localized by surrounding surface. The shape of this surface interface is formed by surface tension of the surrounded liquid to the spherical shape in stabile stage. Bubbles tend to move due to the buoyancy force present and the moving bubble is formed not only by surface tension, but by dynamic property of the liquid, viscosity especially. (Grace 1973,1976) and (Critf *et al* 1978) proposed the bubble-shape map based on three dimensionless numbers: Reynolds, Eötvos and Morton number. Reynolds number is defined:

$$\mathrm{Re} = \frac{\rho d v}{\mu} \ , \tag{12}$$

where d is bubble diameter (m), v is bubble velocity (m.s^{-1}), ρ is liquid density (kg.m^{-3}) and μ is liquid viscosity (kg.m^{-1}.s^{-1}). Eötvos number is defined:

$$Eo = \frac{g\Delta\rho d^2}{\sigma} \ , \tag{13}$$

where g is gravitational acceleration (m.s^{-2}), $\Delta\rho$ is density difference between gas and liquid and σ is surface tension (N.m^{-1}) of the liquid. Morton number is defined:

$$Mo = \frac{g\mu^4\Delta\rho}{\rho^2\sigma^3} \ . \tag{14}$$

The value of this number is independent of bubble dimension. The bubble-shape map based on these three numbers is in the figure 3. It shows the basic shapes of the bubbles. It is shown that all bubbles with Reynolds number less then 1 are spherical. This map can be used for relative maximal velocity determination of not deformed bubble. For example the maximal velocity of not deformed 2 mm bubble in water corresponds to 45 mm/s.

Bubble rising velocity is limited due to the liquid viscosity in the liquid. The final velocity of rising bubble can be de deduced from the Comolet's diagram shown in the figure 4.

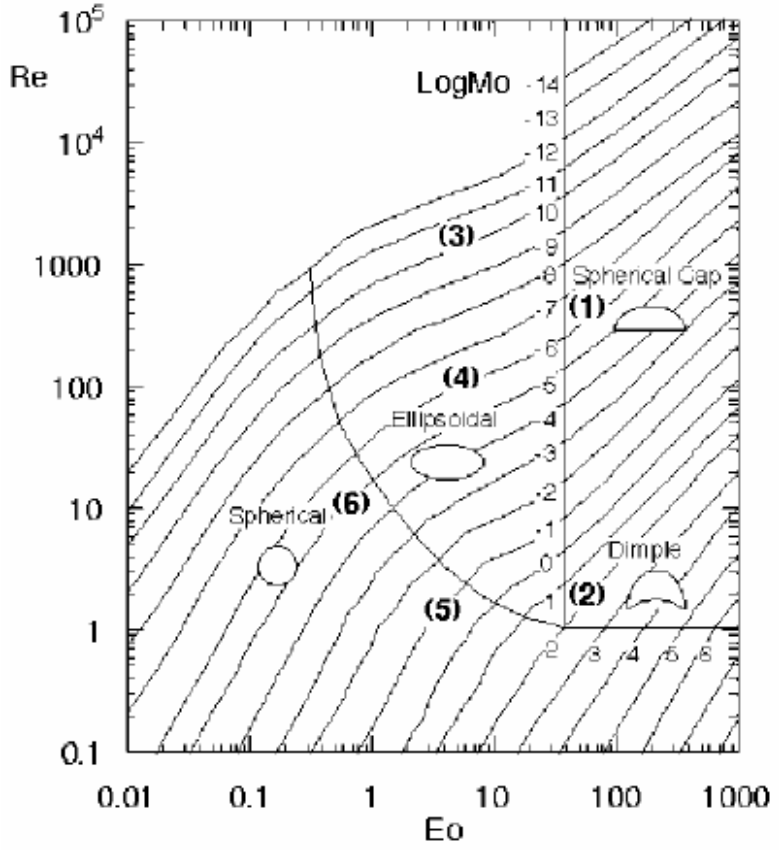

Figure 3 Bubble-shape map.

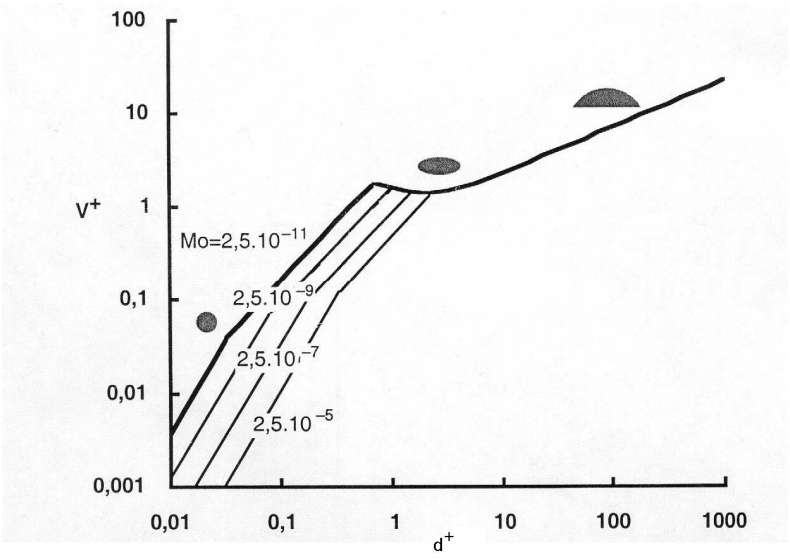

Figure 4 Comolet's diagram.

Parameters V^+ and d^+ are not directly the speed and diameter of the bubble, but they are functions of:

$$V^+ = \left(\frac{g\Delta\rho\sigma}{\sigma^2} \right) V_\infty \text{ and } d^+ = \sqrt{\frac{g\Delta\rho}{\sigma}}\, d \,. \tag{15}$$

From this diagram it can be deduced that all bubbles with a diameter less then 1,6 mm should be always spherical in the water of temperature under 20°C, maximal rising velocity including. Moreover, dimension of always spherical bubble increases for the liquids with higher value of surface tension or viscosity. It means there is a wide range of bubbles suitable for the devised measurement instrument application.

4. Measurement

The goal of the presented measurement is to perform the first bubble position and dimension measurement. A special experimental vessel was designed, constructed and mounted to present experimental method testing. This experimental bottle is using the part of the glass cylindrical tube filled with distilled water like an anamorphotic part of the optical system. Bubble imaginary image is observed with camera equipped by common lens. Optical parameters of this lens had to be proven. Experimental vessel was design to minimize unwanted illumination of the camera pictures caused by total reflection on the spheres objects of main illumination source rays. It is possible to use direct or side-indirect illumination scheme of the observed 3D space to minimize reflections. Experimental vessel was design like top and bottom open in order it was possible to locate any kind of spherical object inside there. Experimental vessel with XYZ movable support is shown in the figure 5.

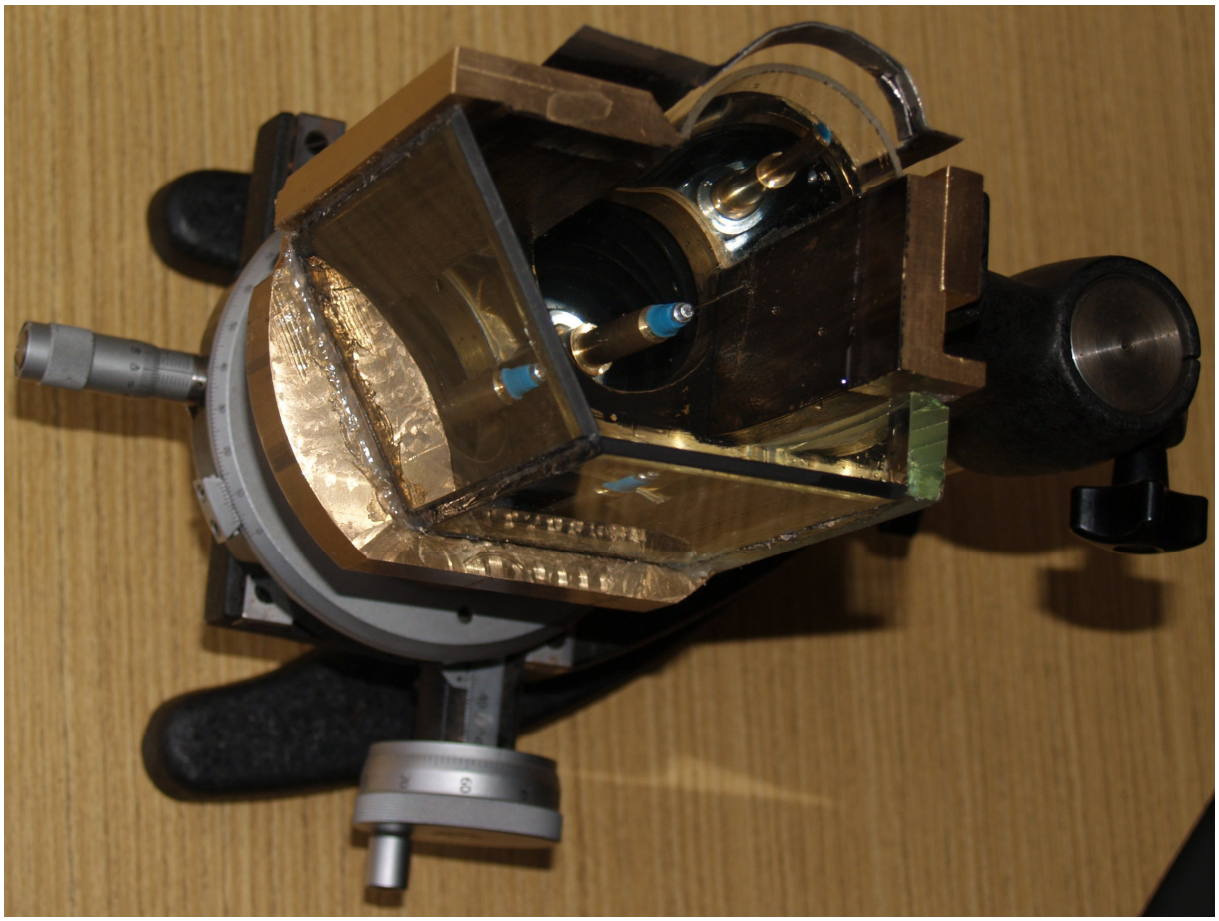

Figure 5 Experimental vessels with XYZ movable support.

In order for results of this experiment to be comparable with the user conditions, the glass tube part used as a cylindrical lens meniscus was made from drawn glass tube. This kind of tube does not have optical quality and it decreases experiment precision. Due to this fact the

radius curvature error of the drawn tube was measured with 3D measurement machine Zeiss. Glass tube profiles shown in the figure 6 were measured in four slices separated by 10 mm.

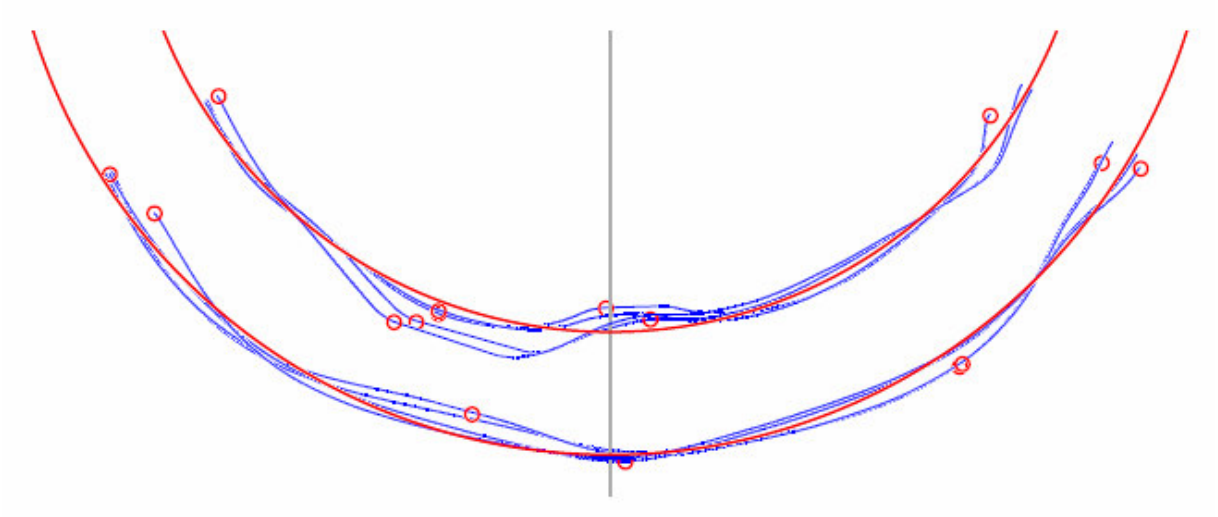

Figure 6 Measured profiles of the used drawn glass tube.

Maximal diameter error was measured to 0,226 mm. We used the right side of the glass tube for the measurement only, where the maximal diameter deviation corresponds to 0,091 mm. This value limits the global accuracy of the application.

Due to this technical complication the precision and repeatability had to be measured. Special X, Y, Z, movable support was used for the precision and repeatability measurement as an auxiliary system of the experimental vessel. The possibility of accuracy and repeatability of the system position determinations was tested by measurement of a glass and steel sphere with diameters 1,62 mm and 2 mm, respectively, mounted on X, Y, Z movable support. Images of the measured volume with spherical object were taken with different camera systems. We used B/W CCD camera, and Olympus E-300 high resolution 8Mpix camera. Captured images were processed with special algorithm written in Matlab for determination X, Y, Z position parameters and radius of each spherical object. These data were compared with the originally adjusted values.

The experimental set-up was arranged as shown in the figure 1c. Experiments show different resolution capability in different directions. For the experimental optical set-up: external radius of cylindrical glass tube R = 25.08 mm with glass thickness t = 1,9 mm, image distance of the camera lens was p´ = 46,7 mm and distance S = 321 mm the Y and Z measurement repeatability and precision was ± 0,035 mm close to the optical axis. Far from the optical axis the repeatability was determined to ± 0,06 mm, but accuracy was affected by offset up to 0,35 mm caused by glass tube radius error. The accuracy in X-axis (along the optical axis) was much lower about ± 3,25 mm. This value is affected with the error of sphere margin manual measurement ± 1,5 pixle. The most precise is determination of the radius of the sphere with error only ± 0,03 mm. It was find that computed radius value is about approximatly 5% smaller then the real value. Expected maximal resolution under the best experimental condition (optical glass quality) is to be estimated: Δy, Δz = 0,02 mm, ΔR = 0,01 mm and Δx = 0,3 mm.

On the base of these results bubbly flow measurement was performed. A needle with a diameter of 0,8 mm was placed to the XYZ movable support instead of sphere of known diameter. The needle was connected with the pressure tank and the air flow to the needle was

controlled by needle valve. Average air flow pressure was approximately 13 kPa. The cause of the released bubble dimension is mainly function of output diameter a capillary tube of inner diameter 70μm was pasted in the needle to decreases rising bubble dimension. Nevertheless produced bubbles are too big to be spherical during all the bubble rising time. Bubble position and radius accuracy determination verification based on known XYZ needle position is limited mainly by variable bubble rising trajectory shown in the figure 7.

Figure 7 Aerial view on the bubble rising trajectory took with exposition times 1/15 s – left and 1 s right.

It means bubble position is in accordance with set needle position when it is in the contact or shortly after it releases capillary tip only.

Spherical object are imaged as ellipsoidal due to the anamorphotic optical system. It is demonstrated in the images of glass sphere placed at different axial position in the figure 8.

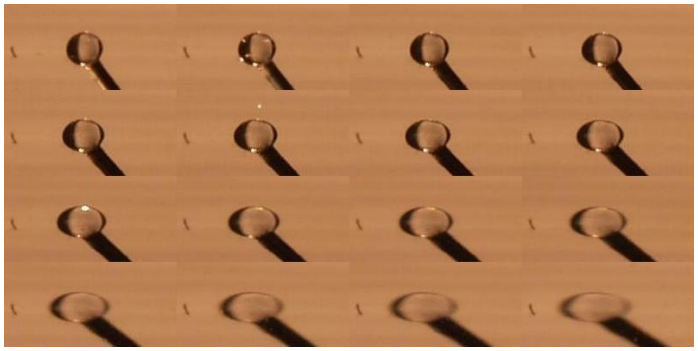

Figure 8 Images of glass sphere inside the cylindrical glass tube filled with water at different axial distances. Axial position difference is 4 mm.

Functionality of the presented method is limited by depth of field sharpness. It can be set to be larger then observed volume, as it is shown in the figure 9, where small spherical bubbles on the both front (circles) and rear (ellipsis) glass wall are observed. Transverse dimension of sharply viewed volume is limited by optical aberration of the used optical system, especially by cylindrical tube. It is demonstrated in the figure 9, where colored spread bubbles on the rear wall cannot be measured yet. Transverse dimension of sharply viewed volume narrows as a function of object plane position along optical axis, as it is shown in the figure 10.

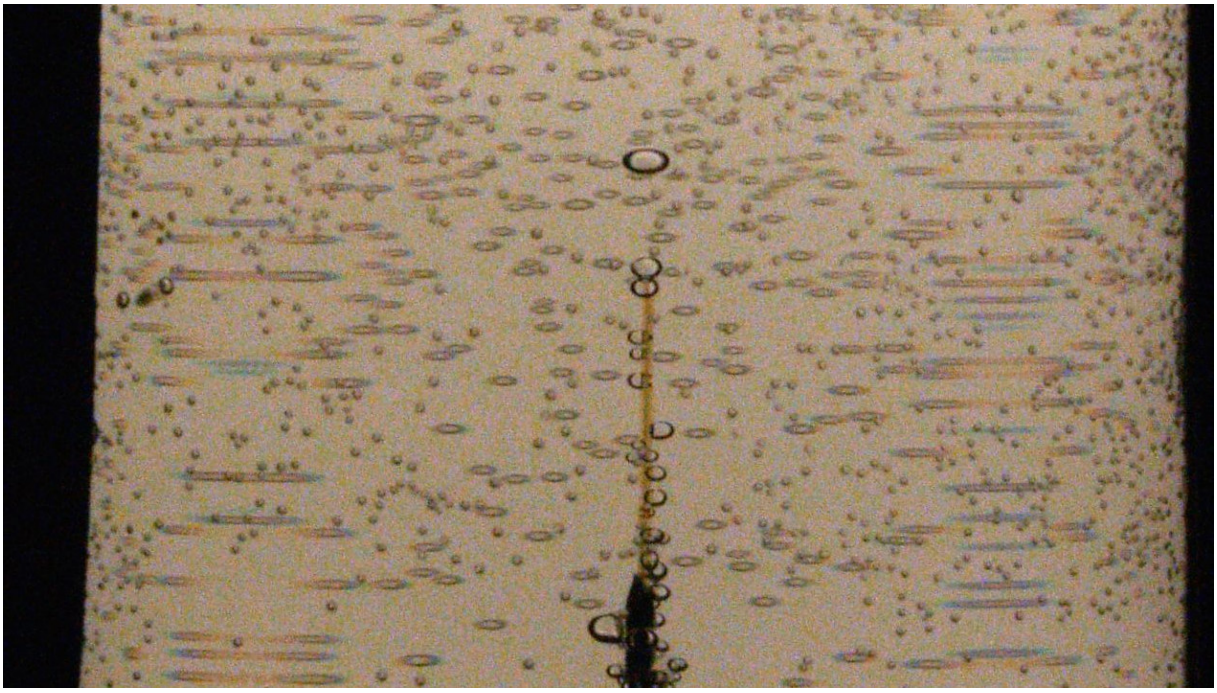

Figure 9 Field of depth in the image is larger then vessel depth equal to 77 mm (much more then glass tube diameter equal to 50,2 mm). Both bubbles attached to the front (circles) and rear (ellipsis) glass wall are observed.

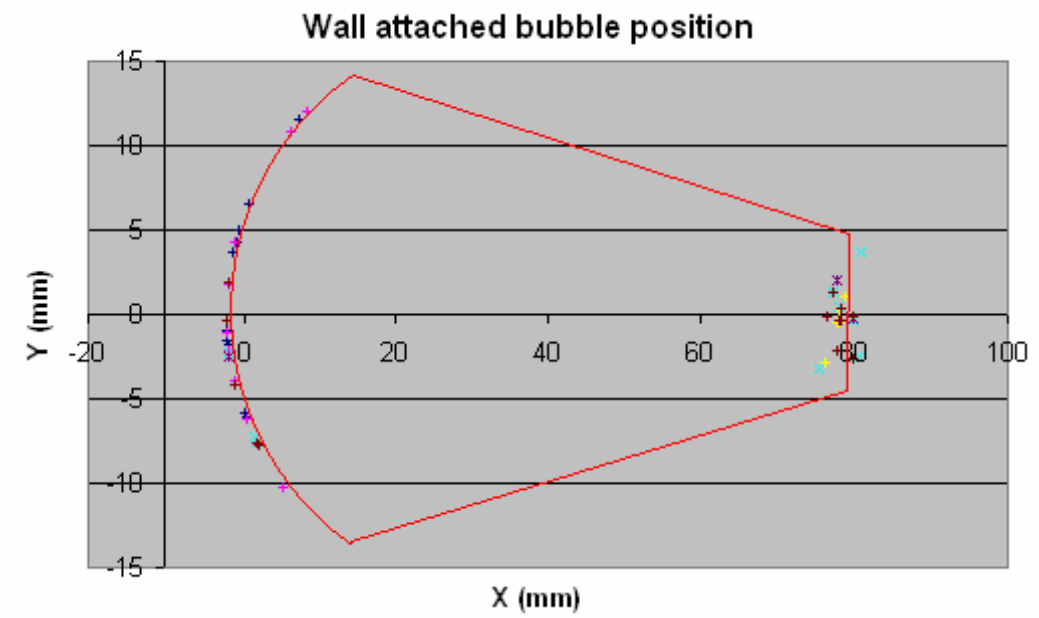

Figure 10 Experimental determined position of chosen wall attached bubbles. Red lines indicate margins of sharply viewed volume.

Bubble diameter was determined to be approximately 1,2 mm, but rising bubble shape was find out to be ellipsoidal during experiments. This experimental complication can be caused by bistability of bubble generation mechanism as it was observed by (Wu, Gharib 1998). Due to this fact, the right bubble position corresponds to the needle set position with similar error as for the previous described measurement used glass and steel sphere glued to needle fixed in XYZ movable support was observed only in the case of bubble attached to the capillary just

before its releases. Random screens images of small spherical bubbles attached to the experimental vessel walls were processed too. Its position well corresponds to the position of front and rear glass wall and average bubble diameter was determined to 0,4 mm, in this case. Temporal increase of bubbles diameter was observed for the series of consecutive snapshots too, as it is shown in the figure 11.

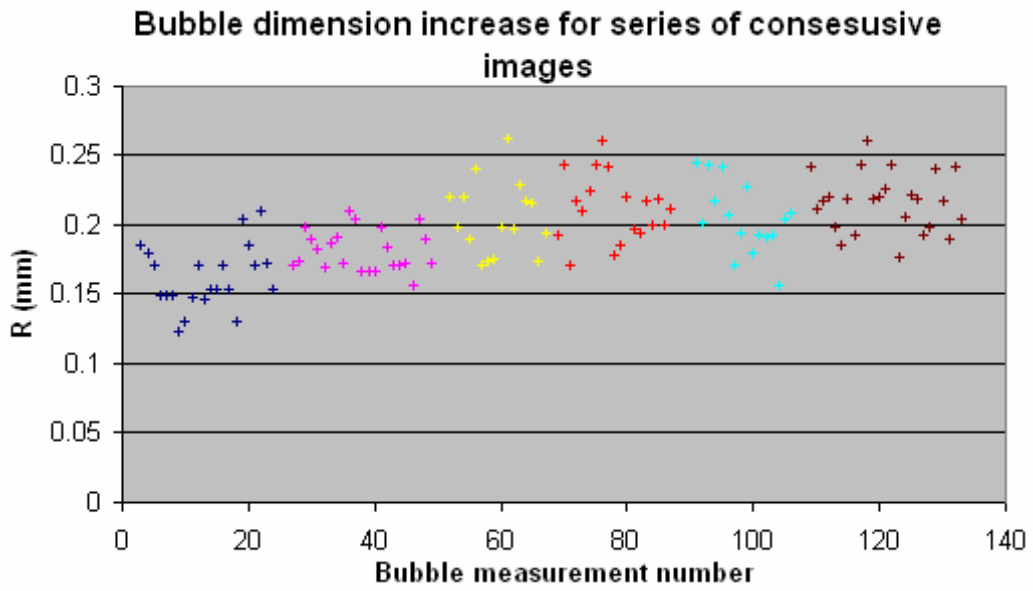

Figure 11 Dimensions of chosen wall attached bubbles of series six consecutive images.

5. Conclusion

The first measurement and data processing are demonstrated in multiphase bubble-liquid system. Bubble measurement was affected by bubble generation problem; where instead of spherical ellipsoidal bubbles were produced. But measurement of bubbles attached to the vessel walls or movable capillary gives resolution similar to measurement of solid glass and steel spheres mounted to movable XYZ support. We expect the presented system will be able to be used for the determination of the spherical objects velocity as well as dimension change in the case of application of time-resolved photography.

6. Acknowledgments

This work was supported by grand CTU 0511212

7. References

Crift, R., Grace, J.R., Weber, M. E. (1978) Bubble drops and particles, in: *Academic Press*, New York, pp. 22-28.

Chanteperdrix, G., Schuler, A. (1999) Two Phase Flows with Fluent B, in: Mastering Industrial Codes and Parallelism REPORTS, http://wn7.enseeiht.fr/hmf/travaux/CD9900/travaux/optmfn/micp/reports/reports.htm.

Grace, J. B. (1973) Shapes and velocities of bubbles rising in infinite liquids, in: *Trans. Int. Chem. Eng.*, 51, 116 – 120.

Grace, J. B. (1976) Shapes and velocities of single drops and bubbles moving freely through immiscible liquids, in: *Trans. Int. Chem. Eng.*, 54, 167 – 173.

Guerrero, J. A., Mendoza, S., Moreno, F., Mfunes-Gallanzi, D., Fernandez-Orozco, S. (2000) Particle positioning from CCD images: experiments and comparison with the generalized Lorenz-Mie theory, in: *Meas. Sci. Technol*. 11 568-575.

Hassan, Y. H. (1997) Multiphase Flow Visualization Utilizing Particle Image Velocimetry (PIV), in: *2nd Int. Workshop on PIV*, Fukui, Japan.

Hošek, J. (2006) Monolens 3-D Imagining and Measurement System, in: *Workshop 2006*, Czech Technical University, Prague.

Jeon, D., Pereira, F., Gharib, M. (2002) Application of DDPIV to Bubbly Flow Measurement, in: *11th International symposium, Application of Laser Techniques to Fluids Mechanics*, Lisbon, Portugal.

Leifer, I., de Leeuw, G., Cohen, L. H. (2003) Optical Measurement of Bubbles: System Design and Application, in: *Journal of Atmospheric and Ocean Technology*, Vol 20, No 9, pp. 1317-1332.

Lindken, R., Merzkirch, W. (2001) A novel PIV technique for measurement in multi-phase flows and its application to two-phase bubbly flows, in: *4th International Symposium on Particle Image Velocimetry*, Göttingen, Germany.

Niwa, Y., Kamiya, Y., Kawaguchi, T., Maeda, M. (2000) Bubble Sizing by Interferometric Laser Imaging, in: *10th International Symposium on Application of Laser Technique to Fluid Mechanics*, Lisbon, Portugal.

Otero, J., Otero, A., Sanchez, L. (2003) 3D motion estimation of bubble gas in fluid glass, using an optical flow gradient technique extended to a third dimension, in: *Machine Vision and Application*, Vol 14, pp. 185-19.

Pan, G., Meng, H. (2002) Digital Holographic PIV for 3D flow measurement, in: *IMECE2002-33173*, New Orleans, Louisiana, November 17-22.

Pereira, F., Gharib, M., Dabiri, D. Modarress, D. (2000) Defocusing digital particle image velocimetry: a 3-component 3-dimensional DPIV measurement technique. Application to bubbly flows, in: *Exp. Fluids* S78-S84.

Pu, Y. Song, X. Meng, H. (2000) Off-axis holographic particle image colorimetric for diagnosing particulate flows, in: *Experiment in Fluids*, S117-S128

Szeliski, R., Kang, S. B. (1993) Recovering 3D Shape and Motion from Image Streams Using Non-Linear Least Squares. Digital Equipment Corporation, Cambridge Research Lab, Cambridge, Messachusetts, USA.

Willert, C. E., Gharib, M. (1992) Three-dimensional particle imagining with a single camera, in: *Exp. Fluids* 12, 353-358.

Wu, M., Gharib, M. (1998) Path instabilities of air bubbles rising in clean water, in: http://arxiv.org/PS_cache/patt-sol/pdf/9804/9804002.pdf